

1 **A high resolution Late Glacial to Holocene record of environmental change**
2 **in the Mediterranean from Lake Ohrid (Macedonia/Albania)**

3 Jack H. Lacey ^{a,d,*}, Alexander Francke ^b, Melanie J. Leng ^{c,d}, Christopher H. Vane ^e, Bernd Wagner ^b

4 ^a Department of Geology, University of Leicester, LE1 7RH, UK

5 ^b Institute for Geology and Mineralogy, University of Cologne, 50674 Köln, Germany

6 ^c Centre for Environmental Geochemistry, School of Geography, University of Nottingham, Nottingham, NG7 2RD, UK

7 ^d NERC Isotope Geosciences Facilities, British Geological Survey, Keyworth, Nottingham, NG12 5GG, UK

8 ^e British Geological Survey, Keyworth, Nottingham, NG12 5GG, UK

9 *Corresponding author. E-mail address: jl237@leicester.ac.uk

10 Keywords: Lake Ohrid, Mediterranean, Holocene, Stable isotopes, Geochemistry, Rock Eval, Palaeolimnology

11 **Abstract**

12 Lake Ohrid (Macedonia/Albania) is the oldest extant lake in Europe and exhibits an outstanding degree
13 of endemic biodiversity. Here, we provide new high resolution stable isotope and geochemical data
14 from a 10 meter core (Co1262) through the Late Glacial to Holocene, and discuss past climate and lake
15 hydrology (TIC, $\delta^{13}\text{C}_{\text{calcite}}$, $\delta^{18}\text{O}_{\text{calcite}}$) as well as the terrestrial and aquatic vegetation response to
16 climate (TOC, TOC/N, $\delta^{13}\text{C}_{\text{organic}}$, Rock Eval pyrolysis). The data identifies 3 main zones: 1) the Late
17 Glacial-Holocene transition represented by low TIC and TOC contents, 2) the early to mid-Holocene
18 characterised by high TOC and increasing TOC/N, and 3) the Late Holocene-Present which shows a
19 marked decrease in TIC and TOC. In general an overall trend of increasing $\delta^{18}\text{O}_{\text{calcite}}$ from 9 ka to
20 present suggests progressive aridification through the Holocene, consistent with previous records from
21 Lake Ohrid and the wider Mediterranean region. Several proxies show commensurate excursions that
22 imply the impact of short-term climate oscillations, such as the 8.2 ka event and the Little Ice Age.
23 This is the best-dated and highest resolution archive of past Late Glacial and Holocene climate from
24 Lake Ohrid and confirms the overriding influence of the North Atlantic in the north-eastern
25 Mediterranean. The data presented set the context for the International Continental scientific Drilling
26 Program (ICDP) Scientific Collaboration On Past Speciation Conditions in Ohrid (SCOPSCO) project
27 cores recovered in spring-summer 2013, potentially dating back into the Lower Pleistocene, and will
28 act as a recent calibration to reconstruct climate and hydrology over the entire lake history.

29 **1. Introduction**

30 Understanding past variation in climate and hydrology in the Mediterranean is vital for establishing
31 future climate scenarios and assessing the potential impact on human populations, as changes in water
32 resources and rainfall are predicted to have important social, economic and political impacts across the
33 region (Giannakopoulos et al. 2009; García-Ruiz et al. 2011). It has been shown that local climate and
34 hydrological change can be defined by stable isotope data from lacustrine carbonates and organic
35 matter (OM) through time (i.e., Leng and Marshall 2004; Leng et al. 2013), and that a regional
36 combination of lake isotope records can be used to assess the spatial coherency of climate change
37 (Roberts et al. 2008).

38 There are numerous stable isotope records from lakes in the Mediterranean (e.g. Zanchetta et al. 2012;
39 Dean et al. 2013; Leng et al. 2013), and several sediment cores have been recovered and analysed from
40 multiple locations within Lake Ohrid (Fig. 1; Roelofs and Kilham 1983; Belmecheri et al. 2009;
41 Wagner et al. 2009; Vogel et al. 2010a; Wagner et al. 2012). The records from Lake Ohrid have shown
42 the lake to provide an archive of long-term climatic and environmental change (e.g. Vogel et al. 2010a)
43 and, in the recent sediments, of changes in nutrient supply from anthropogenic impact (Matzinger et al.
44 2007). However, high-resolution data are needed to better understand rapid climatic variability and
45 anthropogenic activity across the region (Francke et al. 2013). Here we present stable isotope and
46 geochemical data from OM, including carbon isotope composition, Total Organic Carbon and Nitrogen
47 ($\delta^{13}\text{C}_{\text{organic}}$, TOC, TOC/N), Rock Eval data including both Hydrogen Index (HI) and Oxygen Index (OI)
48 and oxygen and carbon isotope composition of calcite ($\delta^{18}\text{O}_{\text{calcite}}$ and $\delta^{13}\text{C}_{\text{calcite}}$) through the Late Glacial
49 to Holocene. Using the combined dataset an interpretation of past climate and environment is discussed
50 and the data are compared with neighbouring lakes Prespa and Dojran, as well as other lakes across the
51 Eastern Mediterranean. The data presented here is the best-dated and highest resolution record from
52 Lake Ohrid for the Late Glacial and Holocene period, and sets the context for the future work on the
53 new ICDP cores that potentially go back at least 1.2 million years (Wagner et al. 2014).

54 **2. General setting**

55 Lake Ohrid (40°54'-41°10'N, 20°38'-20°48'E) is a transboundary lake located within the north-eastern
56 Mediterranean, spanning the border between Macedonia and Albania to the west of the Balkan
57 Peninsula (Fig. 1). It is situated at an altitude of 693 m above sea level (a.s.l.) and is bounded to the
58 west by the Mokra Mountain Chain (1500 m a.s.l.) and to the east by the Galičica Mountain (2262 m
59 a.s.l.) and Mali Thate Mountain Chains (2287 m a.s.l.; Albrecht and Wilke 2008). Lake Ohrid formed
60 in an approximately N-S trending graben towards the end of the Alpine Orogeny during the Pliocene
61 (Aliaj et al. 2001), as a result of extensional tectonics that are still active today (Reicherter et al. 2011;
62 Hoffmann et al. 2012). The lake has a maximum N-S length of 30.8 km, a maximum E-W width of
63 14.8 km and covers an area of 358 km² (Stankovic 1960). The basin has a bathtub-shaped morphology
64 with a maximum water depth of 293 m and an estimated volume of 50.7 km³ (Fig. 1; Popovska and
65 Bonacci 2007). In the deepest parts of the lake sediment accumulation rates are ≈ 0.5 mm year⁻¹
66 (Wagner et al. 2008a).

67 The climate in the region surrounding Lake Ohrid is controlled by both sub-Mediterranean and
68 continental influences (Panagiotopoulos et al. 2013), owing to the lake's position in a deep valley
69 sheltered by the surrounding mountains and its proximity to the Adriatic Sea (Vogel et al. 2010a).
70 Average annual rainfall within the Lake Ohrid watershed is 907 mm and average annual air
71 temperature is +11.1°C, ranging from -5.7°C to +31.5°C (Popovska and Bonacci 2007). North-south
72 winds dominate (>75%) and trace the Ohrid valley, with northerly winds prevailing in autumn-winter
73 and southerly winds in spring-summer (Stankovic 1960).

74 The Lake Ohrid catchment covers an area of around 1002 km² (Popovska and Bonacci 2007), which
75 increases to 2600 km² when aquifer input from neighbouring Lake Prespa is included (Matzinger et al.
76 2006b). Lake Prespa, situated 10 km to the east and 150 m above Lake Ohrid at 849 m a.s.l. (Leng et
77 al. 2013), feeds Lake Ohrid through a network of karst aquifers which account for 55% of water input
78 into the lake (Matzinger et al. 2006a); the remaining 45% of overall input comes from direct
79 precipitation on the lake's surface and river inflow (Albrecht and Wilke 2008). The karst aquifer input
80 comprises 49% sub-lacustrine karst springs and 51% surface springs (Matzinger et al. 2006a; Matter et
81 al. 2010). The main hydrological output from Lake Ohrid is through the River Crn Drim (66%) to the
82 northern shore and the residual third is lost through evaporation and seepage (Matzinger et al. 2006b).

83 The upper 150 m of the lake water is thermally stratified in summer months and mixed through winter;
84 below 150 m the lake is stratified by salinity, only mixing on a sub-decadal cycle (Hadzisce 1966;
85 Matzinger et al. 2006b). Presently Lake Ohrid is oligotrophic with an average Secchi depth of
86 approximately 14 m (Matzinger et al. 2006b).

87 **3. Material and methods**

88 **3.1. Core recovery**

89 A ca. 10 meter sediment core (Co1262) was recovered from a locality to the east of the Lini peninsula
90 (41°03'56.9"N, 020°40'21.9"E) in 260 m water depth during June 2011. The core was retrieved in 2 m
91 long sections from a floating platform using a gravity corer for shallower sediments and a percussion
92 piston corer for deeper sediments, where core recovery approached 100%. The coring location was
93 selected based on hydro-acoustic surveys conducted over the period 2004-2009, primarily to study the
94 link between 'mass wasting' deposits (MWD) and earthquakes (Reicherter et al. 2011). Lindhorst et al.
95 (2014) describe the hydro-acoustic surveys that record information on the sedimentary architecture and
96 bathymetry of Lake Ohrid. These show prominent faults and half-graben structures, where successions
97 of MWD are present (Wagner et al. 2012). Post-recovery the core was split into roughly 1 m long
98 sections and stored in darkness at 4°C. Subsequently the core segments were opened, halved
99 lengthwise, described macroscopically, split into 2 cm segments (total correlated core depth = 10.05 m)
100 and then freeze dried. The concentration of total inorganic carbon (TIC) was determined using a
101 DIMATOC 200 (DIMATEC Co.; Wagner et al. 2012).

102 **3.2. Geochemistry of organic matter**

103 Core Co1262 was sampled for organic geochemistry from the surface to 119 cm (correlated depth)
104 every 2 cm, beneath which a 202 cm thick MWD occurs (Wagner et al. 2012). Samples were then
105 taken at 2 cm intervals from 321 cm to 963 cm to a second MWD (18 cm); below 981 cm sampling
106 continued to the base of the core at 1005 cm. The MWD material is homogenous with no significant
107 changes in TIC or organic content (Wagner et al. 2012), and was not analysed as the horizons represent
108 short-term events that can be considered instantaneous.

109 For the $\delta^{13}\text{C}_{\text{organic}}$ of OM, TOC and N, around 500 mg sample was added to 5% HCl to remove calcite,
110 rinsed in deionised water, dried at 40°C and then transferred to a vial after being ground to a fine
111 powder and homogenised. The samples were combusted using a Costech ECS4010 elemental analyser
112 at approximately 1400°C, and then analysed using a VG Optima dual inlet mass spectrometer.
113 $\delta^{13}\text{C}_{\text{organic}}$ are reported as per mil (‰) deviations of the $^{13}\text{C}/^{12}\text{C}$ ratio calculated to the Vienna Pee Dee
114 Belemnite (VPDB) scale, utilising within-run laboratory and international standards. Analytical
115 reproducibility for the within-run standards was <0.1‰ for $\delta^{13}\text{C}_{\text{organic}}$, <0.7% for TOC and <0.2% for
116 N.

117 For Rock Eval analysis approximately 60 mg of sediment was used. Each sample was heated at 25°C
118 minute^{-1} in an inert atmosphere of N_2 from 300°C up to 650°C, after which the residual carbon was
119 oxidised at 20°C minute^{-1} from 300°C to 850°C. A flame ionisation detector measured the release of
120 hydrocarbons during the two-stage pyrolysis and an infrared cell monitored CO and CO_2 release during
121 thermal cracking of the bound OM. The performance of the instrument was assessed against IFP 160
122 000 and S/N1 5-081840. Rock Eval analysis gives 13 acquisition parameters which are determined by
123 integrating the amounts of OM, CO and CO_2 ; including S1 (hydrocarbons previously generated,
124 distilled out upon heating to 300°C) and S2 (hydrocarbons generated through cracking of bound OM,
125 upon temperature increase to 850°C). This paper presents the HI ($\text{S2} \cdot 100 / \text{TOC}$) and OI
126 ($\text{S3} \cdot 100 / \text{TOC}$), with analytical reproducibility for the within-run standards of HI ± 16 and OI ± 3 .

127 **3.3. Stable isotope analysis of carbonates**

128 The sediments of Co1262 were sampled for $\delta^{18}\text{O}_{\text{calcite}}$ and $\delta^{13}\text{C}_{\text{calcite}}$ at the same resolution as the
129 organic samples to 729 cm. Below 729 cm TIC content decreases to <0.1% (apart from a spike at 775
130 cm; Wagner et al. 2012) to 813 cm and sampling was thereafter carried out at 4 cm intervals. There are
131 small TIC spikes (0.2-2%) at 965 cm to 981 cm, where a MWD horizon is observed (Wagner et al.
132 2012). Samples from two previous Lake Ohrid cores (Co1202 and Lz1120) were analysed by XRD to
133 determine mineralogy of the carbonate (cf. Leng et al. 2010), the TIC was confirmed to be calcite,
134 which is in agreement with observations that have been made using SEM (Lézine et al. 2010; Matter et
135 al. 2010).

136 The subsamples were processed to oxidise reactive organic material by disaggregating around 500 mg
137 of sample in 100 ml of 5% sodium hypochlorite solution for 24 hours. Following this the samples were

138 sieved at 63 μm , which is usually assumed to remove any potential biogenic carbonate (Leng et al.
139 2013). The <63 μm fraction was rinsed three times in deionised water, dried at 40°C and powdered.
140 Once prepared the subsamples were reacted overnight in a vacuum with anhydrous phosphoric acid at a
141 constant 25°C, to evolve the CO_2 for analysis. The CO_2 was analysed using a VG Optima dual inlet
142 mass spectrometer. The mineral-gas fractionation factor used for calcite was 1.01025 (derived from
143 Rosenbaum and Sheppard 1986). $\delta^{18}\text{O}_{\text{calcite}}$ and $\delta^{13}\text{C}_{\text{calcite}}$ are reported as per mil (‰) deviations of the
144 isotopic ratios ($^{18}\text{O}/^{16}\text{O}$ and $^{13}\text{C}/^{12}\text{C}$) calculated to the Vienna Pee Dee Belemnite (VPDB) scale,
145 utilising within-run laboratory and international standards (MCS and CCS). Analytical reproducibility
146 for the within-run standards was <0.1‰ for $\delta^{18}\text{O}_{\text{calcite}}$ and $\delta^{13}\text{C}_{\text{calcite}}$.

147 **4. Results**

148 **4.1. Chronology**

149 The age model for Co1262 is based on 6 radiocarbon ages, 3 tephtras, and cross correlation with
150 published records from Lake Ohrid and nearby Lake Prespa (Table 1; Fig. 2). Wagner et al. (2012)
151 gives an expanded discussion for each dating point and a summary of chronological control. The age-
152 depth model (Fig. 2) for the pelagic sediments of core Co1262 was calculated with the software
153 package CLAM v.2.2 (Blaauw 2010), operating with the IntCal 13 calibration curve (Reimer et al.
154 2013). The age-model was interpolated between the radiocarbon ages, the tephtras and cross correlation
155 points using a smooth spline function (smoothing = 0.1). MWD were not included in the calculations
156 and subtracted from the composite profile.

157 Six radiocarbon ages have been obtained, 5 from terrestrial plant material and 1 using fish remains. The
158 fish remains produce a radiocarbon date of 12,400 cal. yr. BP indicating a much older age than
159 expected (754 cm depth = 9433 cal. yr. BP). A reservoir effect of >1500 years has been documented in
160 previous Lake Ohrid cores (Wagner et al. 2008a; Vogel et al. 2010a), however a discrepancy of 3000
161 years is most likely explained by a combined scenario of reservoir effect and re-deposition. The three
162 tephtras, distinguished in horizons marked by high levels of K and Sr, have been previously well dated
163 in Lake Ohrid (Table 1; Sulpizio et al. 2010; Vogel et al. 2010b). Wagner et al. (2012) describes the
164 major element composition of the tephtra and cryptotephtra for Co1262.

165 The age model for core Co1262 shows a high sedimentation rate of 1.1 mm year^{-1} within the upper and
166 lower sections, reducing to 0.6 mm year^{-1} between 450 cm to 650 cm, and gives a basal age of ca. 12.3
167 ka (Fig. 2). The base of the core reaches back into the last glacial period, which is confirmed by the
168 presence of coarse-grained material (thought to represent ice-rafted debris) and low TIC (Wagner et al.
169 2009, 2012; Vogel et al. 2010a). Due to the variable sedimentation rate (Fig. 2) the constant sample
170 size of 2 cm incorporates differing amounts of climate signal providing a resolution (per centimetre) of
171 approximately 20-40 years in the middle part of the core and a greater resolution of 10-20 years in the
172 lower and upper parts of the core (Fig. 2).

173 **4.2. Organic geochemistry and stable isotope analysis**

174 The Lake Ohrid core Co1262 covers the last 12.3 ka, and therefore spans the transition from the Late
175 Glacial through to the Holocene. In general the sediments comprise greyish-olive homogenous clay to
176 silt grade mud, with minor changes in colour associated with varying TIC and TOC (Fig. 3, Wagner et
177 al. 2012). The sediments are massive and structureless, similar to other Lake Ohrid Holocene
178 sequences, which can be attributed to bioturbation (Wagner et al. 2009; Vogel et al. 2010a). The core
179 features several horizons of increased grain size (sand to gravel) and decreased water content that are
180 thought to represent MWD (Wagner et al. 2012). TOC is minimal ($<1\%$) in the lower part of the core.
181 Higher TOC occurs between 8 ka and 3.5 ka, with a maximum of 7.3% at 5.2 ka. Thereafter, TOC
182 decreases to around 3%. Over the majority of the core TOC results are tracked by TOC/N ratios, where
183 TOC/N ranges from 5.5 to 11.2, excluding a rapid increase at 12 ka and a large excursion to higher
184 values around 0.5 ka. $\delta^{13}\text{C}_{\text{organic}}$ averages -27.5% over the entire record, has elevated values in the
185 upper and lower core sections and decreases to a minimum of -29.0% through the central unit.
186 $\delta^{13}\text{C}_{\text{organic}}$ is generally opposed to TOC and TOC/N. HI values from Rock Eval analysis track changes
187 in TOC/N, having lower values in the upper and lower parts of the core, reaching a maximum of 470 at
188 5.2 ka and a minimum of 57 at 2.0 ka. OI broadly opposes HI but is by comparison relatively constant,
189 except from a spike at 2.0 ka, commensurate with the HI minimum. At the base of the core there are
190 two zones of minimum TIC (below 10.3 ka and between 9.8-9.1 ka) where TIC $<0.5\%$ was difficult to
191 analyse for stable isotopes. Maximum TIC (7.1%) occurs at 4.9 ka, approximately at the same time as
192 maximum TOC, and mirrors high TOC values through the section until 2 ka. From the base of the core
193 to 8.5 ka $\delta^{18}\text{O}_{\text{calcite}}$ values are erratic but generally decrease, fluctuating between -6.5% to $+1.9\%$, then
194 gradually increase by $+2\%$ through the main body of core to the current value of -4.5% . $\delta^{13}\text{C}_{\text{calcite}}$

195 values show a similar range, the maximum value of +1.8‰ being toward the base of the core and the
196 minimum of -3.1‰ at 8.6 ka, where after $\delta^{13}\text{C}_{\text{calcite}}$ remains relatively constant through to present
197 averaging +0.4‰ apart from one prevalent positive excursion from 2 ka to 1.5 ka of +0.9‰. There are
198 several short-term excursions shown across multiple proxies (e.g. 8.2 ka, 3.4 ka, 2.0 ka and 0.5 ka; Fig.
199 3).

200 **5. Discussion**

201 **5.1. Sources of organic matter in the Lake Ohrid sedimentary record based on TOC/N and Rock** 202 **Eval data**

203 The Lake Ohrid sediments show fluctuations in TOC, TOC/N and HI, which generally have an inverse
204 relationship with OI and $\delta^{13}\text{C}_{\text{organic}}$ (Fig. 4). These relationships are seen during both short-term events
205 (e.g. at \approx 8.2 ka or 2.0 ka) and as broad changes that define three main zones (Fig. 3).

206 The OM contained within a lake sediment record represents past changes in organic production,
207 catchment vegetation and the amount of particulate and dissolved material transferred to the lake, as
208 well as degradation and dilution effects resulting from differing abundances of inorganic components
209 (Meyers and Teranes 2001). OM is made up of a compound mixture of lipids, carbohydrates and
210 proteins, amongst other constituents produced by organisms that lived both within the lake and in the
211 surrounding catchment (Meyers 2003). The total autochthonous and allochthonous OM in the
212 sedimentary record may only represent a small fraction of that originally produced due to oxidation
213 during settling prior to its incorporation into the sediment. It is suggested that bulk organic content still
214 retains important source information even if over 90% is lost through degradation (Meyers and Eadie
215 1993; Meyers et al. 1995; Hodell and Schelske 1998). The TOC/N ratio and the HI-OI data especially
216 are used to estimate the origin of OM and ultimately establish whether organic sedimentation was
217 dominated by endogenic or exogenic processes (Talbot and Livingstone 1989; Meyers and Teranes
218 2001).

219 The TOC/N ratio of OM is used to distinguish primary source location differentiated by the separation
220 of vascular and non-vascular plant compositions, TOC/N is lower (generally <10) in aquatic plants
221 (Talbot and Johannessen 1992), whereas TOC/N is higher (>20) in vascular plants (Meyers and
222 Teranes 2001; Leng and Marshall 2004). The TOC/N ratio of Co1262 fluctuates but in general is below

223 10 (Fig. 3), with a mean = 8.8 (± 1.2 , 1σ) ranging between 5.5 and 11.2. TOC/N suggests that aquatic
224 plants (probably phytoplankton) comprise the predominance of OM through the core. However, the
225 lowest TOC/N could be due to selective decomposition (Leng et al. 2010).

226 Rock Eval pyrolysis is used here to identify and characterise potential source components. The most
227 useful derived measurements from Rock Eval pyrolysis for lake studies are the Hydrogen Index (HI)
228 and the Oxygen Index (OI), which are thought to reflect the origin of sedimentary OM (Meyers and
229 Teranes 2001) and compliment TOC/N data. Three main types of OM (Types I, II, III) are
230 distinguished using a van Krevelen-type HI-OI diagram, but these types are also controlled by the
231 degree of oxidation and alteration during thermal maturation (Talbot and Livingstone 1989). Type I
232 sediments arise from material that is rich in hydrocarbons from microbial biomass or waxy land plants,
233 Type II from algal OM and Type III from woody plant material (Meyers and Teranes 2001). The data
234 from Co1262 shows both Type II and Type III OM, which fall on a curve of changing OI suggesting a
235 differential amount of oxidation either as a product of source changes or degradation (Fig. 4e). The
236 curve is not temporally disturbed, so the changes are the result of climate or environmental change at
237 the time of deposition and are not due to a progressive variation (Leng et al. 2013). In general HI and
238 OI are indirectly correlated ($R^2 = 0.5$, Fig. 4e) and mostly represent Type II sediments (higher HI and
239 lower OI). Zones III and I have a small fraction of Type III dominated (low HI and high OI) sediments.
240 HI exhibits much greater variation than OI and also is positively correlated with changes in TOC/N (R^2
241 = 0.6, Fig. 4a), which suggests a dominantly algal source of OM. If organic proxies tracked variations
242 in the amounts of aquatic and terrigenous material in the sediment, due to the compositional variation a
243 positive correlation between TOC/N and OI would be expected and a negative correlation between
244 TOC/N and HI. Major excursions are therefore the likely product of selective degradation, as with low
245 TOC/N (Fig. 4a, 4b), rather than being caused by OM source changes.

246 **5.2. Carbon isotope composition of organic matter from Lake Ohrid**

247 As TOC/N and Rock Eval data suggest the sediment OM to be mostly pure algal material, $\delta^{13}\text{C}_{\text{organic}}$
248 should record past variations in the aquatic carbon cycle (Leng et al. 2010). Even after degradation, as
249 with TOC/N, bulk sediments are thought to retain primary signatures and preserve relative isotope
250 variations (Meyers et al. 1995; Hodell and Schelske 1998). Within hard water lakes, such as Lake
251 Ohrid, algae utilise dissolved HCO_3^- and therefore $\delta^{13}\text{C}_{\text{organic}}$ will likely be a product of changes in the

252 isotopic composition of the dissolved bicarbonate; changes due to fluctuations in productivity rates and
253 surface nutrient availability are also possible (Leng et al. 2013). Secondary effects may be a mixture of
254 variations in pH, temperature and growth rate (Meyers and Teranes 2001). Phytoplankton within the
255 lake will preferentially use ^{12}C to form OM that averages 20‰ lighter than the dissolved inorganic
256 carbon source, and so changes in carbon supply can have a significant effect on $\delta^{13}\text{C}_{\text{organic}}$ (Leng et al.
257 2005). One major carbon source is likely to be isotopically light soil-derived CO_2 ($\delta^{13}\text{C} = -32$ to –
258 20‰) formed by the decay of terrestrial organic matter, however as HCO_3^- is the dominant carbon
259 species ($\delta^{13}\text{C} \approx +10$ ‰ higher than CO_2 ; Meyers and Teranes 2001) the dissolved HCO_3^- $\delta^{13}\text{C}$ should be
260 in the region of –22 to –10‰ (Leng and Marshall 2004). Values from Col262 imply a lake-water
261 $\delta^{13}\text{C}_{\text{DIC}}$ source of approximately –9 to –5‰ as $\delta^{13}\text{C}_{\text{organic}}$ ranges between –29 to –25‰ (Fig. 3), which
262 suggests the bicarbonate pool may have had a secondary more enriched carbon source. A probable
263 origin for the heavier carbon is from the dissolution of the karst aquifer rocks, known to have average
264 $\delta^{13}\text{C} = +1$ ‰ (Leng et al. 2010). Therefore, excursions in $\delta^{13}\text{C}_{\text{organic}}$ through the core most probably
265 correspond to periods of enhanced or reduced soil-derived carbon delivery to the lake. In general
266 $\delta^{13}\text{C}_{\text{organic}}$ is higher in Zone III, decreases through Zone II to a minimum between approximately 5 and
267 3.5 ka, then becomes more variable through Zone I. $\delta^{13}\text{C}_{\text{organic}}$ broadly follows a diversification in
268 catchment arboreal pollen types (expansion of woodland) through the early Holocene and the
269 associated development of rich organic soils (Panagiotopoulos et al. 2013).

270 **5.3. Oxygen isotope composition of calcite from Lake Ohrid**

271 During the spring-summer when lake surface temperatures reach up to 27°C (Matzinger et al. 2006b)
272 calcite will be precipitated in the epilimnion by photoautotrophic organisms that capture the oxygen
273 isotope composition of lake water ($\delta^{18}\text{O}_{\text{lakewater}}$) at a given temperature. Thus $\delta^{18}\text{O}_{\text{calcite}}$ is a function of
274 both the temperature and $\delta^{18}\text{O}_{\text{lakewater}}$ in which it formed (Leng and Marshall 2004). The variation in
275 isotopic composition over time records the evolution of the water body (Talbot 1990). Calcite
276 precipitation requires an adequate supply of Ca^{2+} and HCO_3^- , which in Lake Ohrid is mainly
277 replenished by springs fed from Lake Prespa and concentrated by evaporation (Leng et al. 2013). SEM
278 investigations of the calcite in Lake Ohrid have reported <30 μm idiomorphic calcite crystals (Matter et
279 al. 2010) that are typical of endogenic-type precipitation (Belmecheri et al. 2009; Leng et al. 2010;
280 Lézine et al. 2010).

281 The present day isotopic composition of waters from Lake Ohrid and of springs within the catchment
282 has $\delta^{18}\text{O}$ ranging between -10.2 and $+1.2\text{‰}$ and δD between -69.9 and -12.9‰ (Fig. 5). These data
283 define a local evaporation line (LEL) which is distinct from the global meteoric water line (GMWL)
284 and indicates Lake Ohrid water is evaporating. $\delta^{18}\text{O}_{\text{lakewater}}$ is therefore a function of inflow (from the
285 karst springs and direct rainfall) and water loss through evaporation, meaning any lower magnitude
286 temperature or source variation signal will be unquantifiable (Leng and Marshall 2004). Lake Ohrid
287 has a large water volume of 55 km^3 and a long residence time of 70 years (Matzinger et al. 2006b),
288 which means it has likely reached a steady state where short-term variations in the input and output are
289 subdued. Any changes in lake water isotope composition are therefore the most likely result of low
290 frequency (centennial) climate variations (Leng et al. 2010). In general, within Lake Ohrid high TIC
291 phases have higher $\delta^{18}\text{O}_{\text{calcite}}$ representing a reduced input/evaporation (I/E) ratio, while low TIC phases
292 have lower $\delta^{18}\text{O}_{\text{calcite}}$ from an increased I/E ratio. The amount of climate signal captured within the
293 endogenic calcites is directly a function of the temporal resolution of the sample size, higher frequency
294 variations will be recorded where sedimentation rates are higher.

295 **5.4. Carbon isotope composition of calcite from Lake Ohrid**

296 Modern water data (Fig. 5) show Lake Ohrid to be sensitive to moisture balance (I/E), however the
297 lake displays little covariance between $\delta^{18}\text{O}_{\text{calcite}}$ and $\delta^{13}\text{C}_{\text{calcite}}$ ($R^2 = <0.1$, Fig. 4f) which is normally
298 associated with (open) water bodies that have shorter residence times (Talbot 1990). Generally in
299 evaporating (closed) lakes, $\delta^{18}\text{O}$ variations are primarily related to water balance fluctuations and $\delta^{13}\text{C}$
300 variations are influenced by the preferential outgassing of ^{12}C -rich CO_2 and exchange with atmospheric
301 CO_2 (Talbot and Kelts 1990). Hence it has been suggested that the degree of palaeohydrological
302 closure can be estimated by the extent of $\delta^{18}\text{O}$ and $\delta^{13}\text{C}$ covariance (Talbot 1990). However, this trend
303 is not evident in Co1262 and is unclear across Mediterranean palaeo-lake datasets indicating that
304 covariance is an unreliable gauge of hydrological balance within the region (Roberts et al. 2008; Leng
305 et al. 2010).

306 $\delta^{13}\text{C}_{\text{calcite}}$ within Lake Ohrid is relatively stable through the majority of the core ($< 9 \text{ ka}$; average
307 $\delta^{13}\text{C}_{\text{calcite}} = +0.4 \pm 0.5\text{‰}$, 1σ) with higher and more variable values in the Early Holocene up to $+1.8\text{‰}$.
308 $\delta^{13}\text{C}_{\text{calcite}}$ ranges between -3.1 and $+1.8\text{‰}$ and implies past lake-water $\delta^{13}\text{C}_{\text{TDIC}}$ between -4.1 and
309 $+0.8\text{‰}$ (due to a $+1\text{‰}$ enrichment between calcite and TDIC; Romanek et al. 1992). The extended

310 residence time of lake-water in Lake Ohrid and the relatively invariant $\delta^{13}\text{C}_{\text{calcite}}$ suggest that the
311 bicarbonate has likely reached a steady state indicating long-term stability between source and
312 utilisation (Talbot and Kelts 1990; Leng et al. 2013). We might expect some photosynthetic control on
313 the isotopic composition of the carbon pool due to removal of ^{12}C by aquatic organisms during times of
314 heightened productivity, causing an increase in the isotopic composition of the carbon pool (assuming
315 burial of organic matter; Andrews et al. 1993, Leng et al. 2013). However, as there is no substantial
316 correlation between higher $\delta^{13}\text{C}_{\text{calcite}}$ (or $\delta^{13}\text{C}_{\text{organic}}$) and higher TIC and TOC content, changes in
317 primary productivity are thought to have little effect on $\delta^{13}\text{C}_{\text{TDIC}}$ which is common for lakes with long
318 residence times (Talbot and Kelts 1990). Other processes that could lower $\delta^{13}\text{C}_{\text{TDIC}}$ are limited in
319 karstic region lakes to primarily the oxidation of OM and the input of soil-derived carbon (Leng et al.
320 2013). Oxidation of OM may be responsible for short-term changes in $\delta^{13}\text{C}_{\text{TDIC}}$ (for example between
321 8.5 to 8 ka) where OI increases coincident with lower $\delta^{13}\text{C}_{\text{calcite}}$ and a reduction in both TIC and TOC.

322 **5.5. Late Glacial-Holocene organic matter and hydrological variability from Lake Ohrid**

323 *5.5.1. Late Glacial to Early Holocene (Zone III)*

324 In the first ca. 0.5 ka of Zone III at the base of the core TOC, TOC/N and HI are all low and OI is high
325 commensurate with the presence of gravel-sized grains which most likely represent ice-rafted debris
326 (Wagner et al. 2009, 2012), suggesting that winter temperatures were low, productivity was at a
327 minimum and therefore sedimentation was dominated by clastic input. A hiatus occurs around this time
328 in a previous core (Lz1120) which is thought to be the result of subaquatic currents causing continuous
329 erosion or the prevention of fine-grained sediment accumulation during low lake levels (Wagner et al.
330 2009). The low quantities of OM and TIC in the lowermost section of the core are therefore likely to be
331 the result of a combined scenario of low productivity and dilution due to high clastic input. Enhanced
332 lakewater circulation would also act to oxygenate lake waters, thereby increasing OM degradation and
333 lead to higher OI values and lower HI and TOC/N which represent altered plant material (Talbot and
334 Livingstone 1989). Less oxidation and higher productivity is suggested from 12 ka by decreasing OI
335 and increases in TOC, TOC/N and HI indicating the onset of warmer temperatures.

336 Zone III shows a consistent positive increase across organic proxies (except OI which decreases),
337 although there is a short-term reversal after 10.4 ka which might be due to the dilution of OM

338 components from increased TIC. A rise from 9.8 ka in TOC, TOC/N and HI potentially indicates
339 increased productivity and enhanced preservation of OM; during this period negligible TIC content
340 could be linked to increased organic content and the addition of fresh water to the lake.

341 The interval between 8500 and 8000 cal. year BP (transition from Zone III to Zone II) is characterised
342 by minima in TOC, TOC/N and HI and a peak in OI, alongside higher $\delta^{13}\text{C}_{\text{organic}}$ and relatively low TIC
343 (<2%). Lower TIC, TOC and HI implies a reduction in primary productivity and carbonate
344 precipitation and/or a higher potential for degradation and dissolution in a more oxygenated water
345 column shown by higher OI. The excursions of proxies through this time approach values that are
346 similar to the end of the core during the Late Glacial, where enhanced mixing and colder conditions
347 prevailed (Wagner et al. 2009). Alongside cooling, aridity is suggested by higher $\delta^{13}\text{C}_{\text{organic}}$ possibly the
348 result of a reduction in run-off and the amount of soil-derived carbon delivered to the lake. Increased
349 aridity is also reported from pollen-based reconstructions from Lake Maliq (Albania; Bordon et al.
350 2009) and Tenaghi Philippon (Greece; Pross et al. 2009), where annual precipitation may have
351 decreased by up to 250 mm through this time. The aridity and cooling documented in Lake Ohrid
352 occurs concomitant with negative excursions in Greenland ice core records (indicating cooling;
353 Rasmussen et al. 2007), which are suggested to be the product of a perturbation to the North Atlantic
354 meridional overturning circulation caused by the final drainage of Lake Agassiz into the North Atlantic
355 ('8.2 kyr event'; Törnqvist and Hijma 2012). The record from Lake Ohrid is consistent with previous
356 spatial reconstructions that infer much drier climate conditions for the Balkan Peninsula during a
357 cooling phase in the Northern Hemisphere (Alley et al. 1997; Magny et al. 2003).

358 *5.5.2. Middle Holocene (Zone II)*

359 Within Zone II, TOC and HI have maximum values (at 5.2 ka) where a parallel rise is most likely due
360 to a significant increase in aquatic algal productivity (Lojka et al. 2009). This is more typical of HI-OI
361 Type II sediments (Fig. 4e) and TOC/N>10 suggests a greater preservation of OM or potentially the
362 incorporation of a minor amount of allochthonous material (high TOC/N). Increased rainfall and
363 lakewater freshening is suggested by decreasing $\delta^{18}\text{O}_{\text{calcite}}$, leading to enhanced inwash which is
364 supported by progressively lower $\delta^{13}\text{C}_{\text{organic}}$ resulting from enhanced delivery of soil-derived carbon.

365 An overall decrease is seen in many of the proxies through to Zone I, where TOC becomes increasingly
366 variable after 4.5 ka. The decline in TOC, TOC/N and HI is most likely associated with lower

367 temperatures and increasing aridity after 4 ka, which has been described previously in other Lake Ohrid
368 cores (Wagner et al. 2008b, 2009; Vogel et al. 2010a) and in records from the wider Mediterranean
369 region (e.g. Bar-Matthews et al. 1999; Magny et al. 2009). A short-term rapid decrease in TIC, TOC,
370 TOC/N and HI occurs shortly after 3.4 ka, which is correlated with elevated K and low H₂O content
371 (Wagner et al. 2012) and is likely associated to the deposition of the Etna FL tephra at 3.37 ka (Coltelli
372 et al. 2000).

373 At 2 ka there is a pronounced and rapid excursion within the Co1262 data where TOC drops to <1%,
374 TOC/N to <6, HI to <60 and OI rises to >550. A maxima in OI indicate more extensive oxidation of
375 OM, which is supported by minimum values for TOC/N and HI being the result of decompositional
376 processes rather than source variation (Talbot and Livingstone 1989; Meyers and Ishiwatari 1995) and
377 decreasing $\delta^{13}\text{C}_{\text{calcite}}$ from the recycling of autochthonous OM. At this time anthropogenic impact in the
378 catchment is thought to be enhanced, including significant forest clearance and greater agricultural
379 activity leading to higher erosion rates (Vogel et al. 2010a; Aufgebauer et al. 2012). Greater erosion
380 would lead to an increased delivery of fine grained clastic material to the lake, seen as a K and
381 sedimentation rate peak in Co1262 (Wagner et al. 2012), and also to an enhanced supply of nutrients
382 and OM. This OM would be readily oxidised, causing the release of CO₂ and a decrease in bottom
383 water pH.

384 5.5.3. Late Holocene to Present (Zone I)

385 Following the transition from Zone II to Zone I, TIC and TOC are generally higher through to roughly
386 0.5 ka, which suggests an increase in productivity and a reduction in both mixing and decomposition of
387 OM. Around this time there was a substantial lake level drop in nearby Lake Prespa, which could have
388 had a profound effect on Lake Ohrid's productivity as waters delivered through karstic springs contain
389 significant amounts of bioavailable elements such as phosphorous (Matzinger et al. 2006a). Reduction
390 of the water level of Lake Prespa may lead to an increased trophic state in Lake Ohrid and the potential
391 for an enhanced phosphorous load to be transferred (Matzinger et al. 2006a; Wagner et al. 2009). There
392 is an associated K decrease in Co1262 through this interval (Wagner et al. 2012), which could be
393 related to increased catchment vegetation reducing erosion; as shown by higher AP percentages in
394 pollen data from Lz1120 (Lake Ohrid; Wagner et al. 2009) and Co1215 (Lake Prespa; Aufgebauer et
395 al. 2012). This may also be related to a decrease in recharge and increased aridity associated with a

396 minor elevation in summer temperatures, indicated by pollen-based reconstructions from Lake Maliq
397 (Bordon et al. 2009), which can be correlated to a warmer climate during the Medieval Warm Period
398 (≈ 1 to 0.7 ka; Crowley and Lowery 2000). Lower values for TIC and TOC after 0.5 ka indicate reduced
399 primary productivity and a slight elevation in OI suggests a return to more oxygenating conditions and
400 an associated increase in OM decomposition. These observations correlate with colder temperatures
401 attributed to the Little Ice Age, observed in other records from Lake Ohrid and the surrounding region
402 (Wagner et al. 2009; Aufgebauer et al. 2012; Francke et al. 2013).

403 In recent years (< 0.15 ka) OM concentrations have started to increase, which may be the result of
404 anthropogenic eutrophication (Matzinger et al. 2007). However, the changes seen during the Late
405 Holocene show that a signal of natural climate variability is preserved within the lake sediments and
406 has not been completely overridden by anthropogenic activity.

407 **5.6. Comparison of oxygen isotope composition between Lake Ohrid and other eastern** 408 **Mediterranean lakes**

409 *5.6.1. Late Glacial to Holocene Transition*

410 High $\delta^{18}\text{O}_{\text{calcite}}$ through the Younger Dryas is seen across Mediterranean lake records (e.g. Lake Van,
411 Wick et al. 2003; Lake Frassino, Baroni et al. 2006), which may be linked to aridity associated with
412 North Atlantic Heinrich events (Roberts et al. 2008). In Lake Ohrid previous studies have suggested
413 low lake levels coincident with stronger wind intensities (Vogel et al. 2010a) and higher $\delta^{18}\text{O}_{\text{calcite}}$ is
414 seen both Lake Ohrid and Lake Prespa (Fig. 6a). This is interpreted as a reduction in winter rainfall and
415 greater summer aridity, conditions characteristic of the Younger Dryas where annual precipitation
416 decreased by up to 50% across the Aegean region (Kotthoff et al. 2011).

417 *5.6.2. Early Holocene*

418 After the Younger Dryas high $\delta^{18}\text{O}_{\text{calcite}}$ phase (post-10 ka), $\delta^{18}\text{O}_{\text{calcite}}$ are at a minimum. This change is
419 common across almost all Mediterranean lakes (e.g. Lake Eski Acigöl and Lake Zeribar; Fig. 6b) and
420 is probably linked to increased freshwater input due to warmer and wetter conditions during the early
421 Holocene, also recorded as a negative shift of ca. 4‰ in Soreq cave speleothems (Bar-Matthews et al.
422 2003). This is also seen as a maximum lake level in the Dead Sea (Frumkin 1997) and wetter
423 conditions as recorded in $\delta^{18}\text{O}$ of land snail shells (Goodfriend 1991). This low $\delta^{18}\text{O}$ phase is

424 coincident with the formation of marine sapropel I in the Mediterranean Sea, which is considered to
425 originate from greater precipitation rates causing freshening of surface waters (Kallel et al. 1997;
426 Kotthoff et al. 2008) combined with increased inflow from the river Nile both acting to create a
427 freshwater surface layer and subsequent bottom water anoxia between 9.5 and 6.5 ka in the
428 Mediterranean Sea (Rohling 1994; Ariztegui et al. 2000). During this time other lakes from around the
429 Mediterranean remain isotopically fresh, shown by relatively sustained low $\delta^{18}\text{O}$ values (Fig. 6b;
430 Roberts et al. 2008).

431 There is a shift to more positive $\delta^{18}\text{O}_{\text{calcite}}$ values in Lake Ohrid between 8.6 ka and 8 ka suggesting
432 increased aridity; at this time lakes Prespa, Gölhisar and Zeribar show exemplified shifts likely due to
433 their shorter lake-water residence times and lower lake water volumes (Stevens et al. 2001; Eastwood
434 et al. 2007; Leng et al. 2013). These positive $\delta^{18}\text{O}_{\text{calcite}}$ are most likely linked to a drier climate in
435 northern and southern Europe during the North Atlantic '8.2 event' (Alley et al. 1997), as part of a
436 hydrological tri-partition at the time (Magny et al. 2003).

437 5.6.3. Middle Holocene

438 Lake Ohrid had less winter recharge from 7 ka, suggested by a general increase in $\delta^{18}\text{O}_{\text{calcite}}$ assuming
439 summer evaporation was not counteracted. This is in contrast to Lake Prespa where recharge was
440 sufficient due to a lower lakewater volume to catchment area ratio (Leng et al. 2010). At Lake Gölhisar
441 $\delta^{18}\text{O}_{\text{calcite}}$ also increases through this time period, however, there is also a higher degree of variability as
442 the lake responds very rapidly to moisture balance changes (Eastwood et al. 2007). Lake Eski Acigöl
443 and Lake Zeribar shift to higher $\delta^{18}\text{O}_{\text{calcite}}$ values from around 7 ka (Roberts et al. 2001; Stevens et al.
444 2001). At Lake Dojran $\delta^{18}\text{O}_{\text{calcite}}$ values remain relatively constant from 7 ka (Francke et al. 2013), but
445 have lower $\delta^{18}\text{O}_{\text{calcite}}$ prior to this, which is most likely due to the shallow bathymetry of the lake. A
446 minor drop in lake level results in a large drop in surface area greatly reducing evaporation leading to
447 lower $\delta^{18}\text{O}_{\text{calcite}}$ (Francke et al. 2013). Overall though, eastern Mediterranean lakes have low and stable
448 $\delta^{18}\text{O}_{\text{calcite}}$ values through the middle Holocene, with variable $\delta^{18}\text{O}_{\text{calcite}}$ due to site specific variations
449 (Fig. 6; Zanchetta et al. 2007a; Roberts et al. 2008; Develle et al. 2010; Leng et al. 2013).

450 Generally high $\delta^{18}\text{O}_{\text{calcite}}$ values are seen between 6 ka and 4 ka in Lake Gölhisar and Lake Zeribar
451 (Stevens et al. 2001; Eastwood et al. 2007), with a shorter-term event recorded in Lake Prespa, Dojran
452 and Eski Acigöl between 4.3 ka and 3.9 ka (Roberts et al. 2001; Francke et al. 2013; Leng et al. 2013).

453 This might correlate to the 4.2 ka event, described previously from the OM data in Lake Ohrid (Section
454 5.5.2), which has been interpreted as a short period of cooler temperatures and more arid conditions
455 comparable to other Mediterranean records (e.g. Bar-Matthews et al. 1999; Magny et al. 2009; Vogel et
456 al. 2010a). Temperature reconstructions from the surrounding Aegean (Rohling et al. 2002) and
457 Adriatic Seas (Sangiorgi et al. 2003) concur with cooling, whilst dry conditions are promoted by
458 reduced moisture availability from the Atlantic during positive North Atlantic Oscillation (Lamy et al.
459 2006) which is correlated with a strong drop in African lake levels resulting from a weakening of the
460 African monsoon (Kröpelin et al. 2008; Magny et al. 2009).

461 5.6.4. Late Holocene

462 Lake Ohrid shows sustained high $\delta^{18}\text{O}_{\text{calcite}}$ from 2 ka until around 0.5 ka which is also recorded across
463 a range of Mediterranean lakes (Roberts et al. 2008) and speleothems (Bar-Matthews et al. 2000;
464 Zanchetta et al. 2007b). Notable, is the large positive excursion in Lake Prespa interpreted as the result
465 of a significant lake level drop (see Section 5.5.3.; Leng et al. 2010). Leading up to and through this
466 time period Northern Europe was cooler due to a decrease in solar insolation (Van Geel et al. 2000;
467 Wanner et al. 2008), which may have caused the pattern of regional aridification by reducing moisture
468 advection from the Atlantic (Leng et al. 2013). This is also seen in a weakening of the African
469 monsoon and the onset of dry conditions in the Sahara (Gasse 2000).

470 Fresher lake-water conditions are suggested from 0.5 ka by lower $\delta^{18}\text{O}_{\text{calcite}}$ in Co1262, however not to
471 the extent of other Lake Ohrid and Lake Prespa records (Vogel et al. 2010a; Wagner et al. 2010; Leng
472 et al. 2013). The degree of freshening may in part be related to changes in Lake Prespa, which for this
473 time had $\delta^{18}\text{O}_{\text{calcite}}$ of $\approx -7\text{‰}$; these waters would have been transferred to Lake Ohrid through the karst
474 aquifer network. An overall freshening of the lake might also be associated with forest clearance and
475 anthropogenic change (Wagner et al. 2009), where a more direct route for rainfall from catchment to
476 lake would result in lake waters reflecting lower $\delta^{18}\text{O}_{\text{rainfall}}$. In recent years apparent freshening has
477 been enhanced where changes in water balance have been anthropogenically controlled by the use of
478 tributaries for agricultural irrigation (Matzinger et al. 2006b) and the 1962 diversion of the River
479 Sateska into Lake Ohrid (Leng et al. 2010).

480 **6. Conclusions**

481 Here, new stable isotope and geochemical data from core Co1262 (the highest resolution and best dated
482 record from Lake Ohrid to date) provides valuable information on local climate and hydrological
483 variations through the Late Glacial to Holocene.

484 The sedimentary sequence from Lake Ohrid have been divided into three main zones based mainly on
485 changes in the organic and inorganic content of the sediments. The lowermost part of Zone III (>12 ka)
486 suggests low productivity and reduced groundwater recharge. The lake-water would have been well
487 oxygenated promoting OM degradation. Warmer temperatures through the rest of this zone might have
488 been the cause of increased lacustrine and catchment productivity. At the transition from Zone III to
489 Zone II an event between 8.6 and 8.0 ka suggests a return to colder conditions and lower productivity,
490 most likely the response in Lake Ohrid to the 8.2 ka cooling event. Zone II shows an initial increase in
491 aquatic productivity and terrestrial input through a warm and stable period. From 4.5 ka OM content
492 becomes more variable following lower temperatures and aridity, a prevalent negative excursion occurs
493 after 3.4 ka coincident with the deposition of the Etna FL tephra. Within an overall change to more
494 positive $\delta^{18}\text{O}_{\text{calcite}}$ (greater aridity) through the Holocene are several rapid arid events, which due to
495 confidence in the dating, appear to match temporally with concomitant excursions in Lake Prespa. A
496 significant short-term excursion is recorded at 2 ka across all datasets to pre-Holocene levels. At this
497 time anthropogenic activity is documented to have had a widespread influence on catchment vegetation
498 through forest clearance leading to higher erosion. Short-term climate variations are seen in the most
499 recent record, in particular increased productivity around 1 ka and the subsequent decrease likely
500 represents the response to the Medieval Warm Period and the Little Ice Age. Recent increases in OM
501 concentrations are probably linked to anthropogenic eutrophication.

502 The data from Co1262 fits both temporally and spatially into what is known about Late Glacial to
503 Holocene climate across the Mediterranean but both at a higher resolution and with a better
504 chronology. The data and interpretations will give context for a reconstruction of climate and
505 hydrology for the SCOPSCO cores over the entire lake history, which likely goes back to the mid
506 Pleistocene (Wagner et al. 2014).

507 **Acknowledgements**

508 The study was funded by the German Research Foundation (WA 2109/11) and by the International
509 Continental scientific Drilling Program (ICDP); it forms part of the PhD research (of JHL) funded by
510 the British Geological Survey University Funding Initiative (BUFI) and also the PhD (of AF) in
511 Cologne. Thanks go to Andrea Snelling and Chris Kendrick for help and training with the isotope
512 analysis.

513 **Figures**

514 **Fig. 1 a and b** Map of the north-eastern Mediterranean showing the location of Lake Ohrid, Lake
515 Prespa and other key sites mentioned in the text, including (1) Lake Dojran, (2) Lake Gölhisar, (3)
516 Lake Eski Acigöl, (4) Lake Zeribar. **c** Bathymetry of Lake Ohrid (defined by 50 m isolines) showing
517 river input/output and the location of coring sites Co1202 (Vogel et al. 2010a), Core 9 (Roelofs and
518 Kilham 1983), Co1262 (this study; Wagner et al. 2012), Lz1120 (Wagner et al. 2009), and JO2004-1
519 (Belmecheri et al. 2009). 1c modified from Vogel et al. (2010a), Fig. 2b

520 **Fig. 2** Age-depth model of core Co1262 based on 3 tephra geochemical correlations, 6 calibrated
521 radiocarbon ages derived from terrestrial plant and fish material and cross correlation of physical
522 parameters, such as TIC, with previous Lake Ohrid and Lake Prespa cores. Accumulation rate (cm
523 year⁻¹) was calculated between known dates using correlated core depths (cm). Wagner et al. (2012)
524 describes the correlation to other Lake Ohrid and Lake Prespa cores in full. Blue radiocarbon curves
525 represent the most probable distribution of calibrated ages. Green tephra markers display a Gaussian
526 distribution of calibrated age error (Table 1). MWD found at 121-319, 346-350, 545-549 and 960-980
527 cm are shown as light grey bands

528 **Fig. 3** Multi-proxy data from Lake Ohrid core Co1262. The data fall into 3 main zones (I, II and III;
529 dashed lines). The chronology is based upon dates given in Table 1 and shown in the age model (Fig.
530 2). $\delta^{18}\text{O}_{\text{calcite}}$ and $\delta^{13}\text{C}_{\text{calcite}}$ 'no data' horizons are due to low calcite content (TIC < 0.5%)

531 **Fig. 4** Cross-plots of **a** TOC/N vs. HI, **b** TOC/N vs. OI, **c** TOC/N vs. $\delta^{13}\text{C}_{\text{organic}}$, **d** TOC vs. HI, **e** HI vs.
532 OI and **f** $\delta^{18}\text{O}_{\text{calcite}}$ vs. $\delta^{13}\text{C}_{\text{calcite}}$. Blue dots = Zone I (0 – 2 ka), red dots = Zone II (2 – 8 ka) and green
533 dots = Zone III (8 – 12.3 ka). R^2 values for each plot and zone are given in Table 2. **e** shows OM from

534 Lake Ohrid on a van Krevelen-type discrimination plot with thermal alteration pathways for OM Types
535 I, II and III, and alteration pathway of Type I and II material during oxidation to Type III (grey dashed
536 lines; after Meyers and Lallier-Verges 1999)

537 **Fig. 5** The isotope composition ($\delta^{18}\text{O}$ and δD) of modern waters from Lake Ohrid and several
538 surrounding springs; the Global Meteoric Water Line (GMWL) and the Local Meteoric Water Line
539 (LMWL) are shown as well as the Local Evaporation Line (LEL) characterised by the isotopic
540 composition of present day lake waters (Leng et al. 2010 and references therein)

541 **Fig. 6 a** Comparison of $\delta^{18}\text{O}_{\text{calcite}}$ between core Co1262 and previous records from Lake Ohrid and
542 Lake Prespa **b** Comparison of $\delta^{18}\text{O}_{\text{calcite}}$ between Co1262 and other records from the eastern
543 Mediterranean region (Fig. 1; Ohrid Co1202, Vogel et al. 2010a; Ohrid Lz1120, Wagner et al. 2010;
544 Prespa Co1215, Leng et al. 2013; Dojran, Francke et al. 2013; Gölhisar, Eastwood et al. 2007; Eski
545 Acigöl, Roberts et al. 2001; Zeribar, Stevens et al. 2001); dashed lines indicate zones described in this
546 paper (Fig. 3)

547 **Table 1** Calibrated radiocarbon and tephra ages used in the age model for core Co1262. The calibration
548 of radiocarbon ages is based on Calib 6.1.1 (Stuiver and Reimer 1993) and INTCAL09 (Reimer et al.
549 2009) and on a 2σ uncertainty (Wagner et al. 2012)

550 **Table 2** R^2 values for cross-plots shown in Fig. 4 calculated within Zone I = 0 – 2 ka, Zone II = 2 – 8
551 ka, Zone III = 8 – 12.3 ka and Whole Core = 0 – 12.3 ka

552 **References**

- 553 Albrecht C, Wilke T (2008) Ancient Lake Ohrid: biodiversity and evolution. *Hydrobiologia* 615
554 (1):103-140
- 555 Aliaj S, Baldassarre G, Shkupi D (2001) Quaternary subsidence zones in Albania: some case studies.
556 *Bull Eng Geol Env* 59 (4):313-318
- 557 Alley RB, Mayewski PA, Sowers T, Stuiver M, Taylor KC, Clark PU (1997) Holocene climatic
558 instability: A prominent, widespread event 8200 yr ago. *Geology* 25 (6):483-486

559 Andrews JE, Riding R, Dennis PF (1993) Stable isotopic compositions of Recent freshwater
560 cyanobacterial carbonates from the British Isles: local and regional environmental controls.
561 *Sedimentology* 40 (2):303-314

562 Ariztegui D, Asioli A, Lowe JJ, Trincardi F, Vigliotti L, Tamburini F, Chondrogianni C, Accorsi CA,
563 Bandini Mazzanti M, Mercuri AM, Van Der Kaars S, McKenzie JA, Oldfield F (2000)
564 Palaeoclimate and the formation of sapropel S1: Inferences from Late Quaternary lacustrine
565 and marine sequences in the central Mediterranean region. *Palaeogeography,*
566 *Palaeoclimatology, Palaeoecology* 158 (3-4):215-240

567 Aufgebauer A, Panagiotopoulos K, Wagner B, Schaebitz F, Viehberg FA, Vogel H, Zanchetta G,
568 Sulpizio R, Leng MJ, Damaschke M (2012) Climate and environmental change in the Balkans
569 over the last 17 ka recorded in sediments from Lake Prespa (Albania/F.Y.R. of
570 Macedonia/Greece). *Quaternary International* 274:122-135

571 Bar-Matthews M, Ayalon A, Gilmour M, Matthews A, Hawkesworth CJ (2003) Sea-land oxygen
572 isotopic relationships from planktonic foraminifera and speleothems in the Eastern
573 Mediterranean region and their implication for paleorainfall during interglacial intervals.
574 *Geochimica et Cosmochimica Acta* 67 (17):3181-3199

575 Bar-Matthews M, Ayalon A, Kaufman A (2000) Timing and hydrological conditions of Sapropel
576 events in the Eastern Mediterranean, as evident from speleothems, Soreq cave, Israel.
577 *Chemical Geology* 169 (1-2):145-156

578 Bar-Matthews M, Ayalon A, Kaufman A, Wasserburg GJ (1999) The Eastern Mediterranean
579 paleoclimate as a reflection of regional events: Soreq cave, Israel. *Earth and Planetary Science*
580 *Letters* 166 (1-2):85-95

581 Baroni C, Zanchetta G, Fallick AE, Longinelli A (2006) Mollusca stable isotope record of a core from
582 Lake Frassino, northern Italy: hydrological and climatic changes during the last 14 ka. *The*
583 *Holocene* 16 (6):827-837

584 Belmecheri S, Namiotko T, Robert C, von Grafenstein U, Danielopol DL (2009) Climate controlled
585 ostracod preservation in Lake Ohrid (Albania, Macedonia). *Palaeogeography,*
586 *Palaeoclimatology, Palaeoecology* 277 (3-4):236-245

587 Blaauw M (2010) Methods and code for 'classical' age-modelling of radiocarbon sequences.
588 *Quaternary Geochronology* 5:512-518

589 Bordon A, Peyron O, Lézine A-M, Brewer S, Fouache E (2009) Pollen-inferred Late-Glacial and
590 Holocene climate in southern Balkans (Lake Maliq). *Quaternary International* 200:19–30

591 Crowley TJ, Lowery TS (2000) How warm was the Medieval Warm Period? *Ambio* 29 (1):51-54

592 Dean JR, Jones MD, Leng MJ, Sloane HJ, Roberts CN, Woodbridge J, Swann GEA, Metcalfe SE,
593 Eastwood WJ, Yiğitbaşıoğlu H (2013) Palaeo-seasonality of the last two millennia
594 reconstructed from the oxygen isotope composition of carbonates and diatom silica from Nar
595 Gölü, central Turkey. *Quaternary Science Reviews* 66:35-44

596 Develle AL, Herreros J, Vidal L, Surssock A, Gasse F (2010) Controlling factors on a paleo-lake
597 oxygen isotope record (Yammoûneh, Lebanon) since the Last Glacial Maximum. *Quaternary
598 Science Reviews* 29 (7-8):865-886

599 Eastwood WJ, Leng MJ, Roberts N, Davis B (2007) Holocene climate change in the eastern
600 Mediterranean region: a comparison of stable isotope and pollen data from Lake Gölhisar,
601 southwest Turkey. *Journal of Quaternary Science* 22 (4):327-341

602 Francke A, Wagner B, Leng MJ, Rethemeyer J (2013) A Late Glacial to Holocene record of
603 environmental change from Lake Dojran (Macedonia, Greece). *Climate of the Past* 9 (1):481-
604 498

605 Frumkin A (1997) The Holocene history of Dead Sea levels. In: Niemi TM, Ben-Avraham Z, Gat JR
606 (eds) *The Dead Sea: The Lake and Its Setting*. Oxford Monographs on Geology and
607 Geophysics 36. Oxford University Press, Oxford:237–248

608 García-Ruiz JM, López-Moreno JI, Vicente-Serrano SM, Lasanta-Martínez T, Beguería S (2011)
609 Mediterranean water resources in a global change scenario. *Earth-Science Reviews* 105 (3-4):
610 121-139

611 Gasse F (2000) Hydrological changes in the African tropics since the Last Glacial Maximum.
612 *Quaternary Science Reviews* 19 (1-5):189-211

613 Giannakopoulos C, Le Sager P, Bindi M, Moriondo M, Kostopoulou E, Goodess CM (2009) Climatic
614 changes and associated impacts in the Mediterranean resulting from a 2°C global warming.
615 *Global and Planetary Change* 68 (3):209-224

616 Goodfriend GA (1991) Holocene trends in $\delta^{18}O$ in land snail shells from the Negev Desert and their
617 implications for changes in rainfall source areas. *Quaternary Research* 35 (3, 1):417-426

618 Hadzisce S (1966) Das Mixophänomen im Ohridsee im Laufe der Jahre 1941/42–1964/65.
619 Verhandlungen des Internationalen Verein Limnologie 16:134-138

620 Hodell DA, Schelske CL (1998) Production, sedimentation, and isotopic composition of organic matter
621 in Lake Ontario. *Limnology and Oceanography* 43 (2):200-214

622 Hoffmann N, Reicherter K, Grützner C, Hürtgen J, Rudersdorf A, Viehberg FA, Wessels M (2012)
623 Quaternary coastline evolution of Lake Ohrid (Macedonia/Albania). *Central European Journal*
624 *of Geosciences* 4 (1):94-110

625 Kallel N, Paterne M, Duplessy JC, Vergnaud-Grazzini C, Pujol C, Labeyrie L, Arnold M, Fontugne M,
626 Pierre C (1997) Enhanced rainfall in the Mediterranean region during the last Sapropel Event.
627 *Oceanologica Acta* 20 (5):697-712

628 Kotthoff U, Koutsodendris A, Pross J, Schmiedl G, Bornemann A, Kaul C, Marino G, Peyron O,
629 Schiebel R (2011) Impact of Lateglacial cold events on the northern Aegean region
630 reconstructed from marine and terrestrial proxy data. *Journal of Quaternary Science* 26 (1):86-
631 96

632 Kotthoff U, Muller UC, Pross J, Schmiedl G, Lawson IT, van de Schootbrugge B, Schulz H (2008)
633 Lateglacial and Holocene vegetation dynamics in the Aegean region: an integrated view based
634 on pollen data from marine and terrestrial archives. *The Holocene* 18 (7):1019-1032

635 Kröpelin S, Verschuren D, Lézine AM, Eggermont H, Cocquyt C, Francus P, Cazet JP, Fagot M,
636 Rumes B, Russell JM, Darius F, Conley DJ, Schuster M, Von Suchodoletz H, Engstrom DR
637 (2008) Climate-driven ecosystem succession in the Sahara: The past 6000 years. *Science* 320
638 (5877):765-768

639 Lamy F, Arz HW, Bond GC, Bahr A, Pätzold J (2006) Multicentennial-scale hydrological changes in
640 the Black Sea and northern Red Sea during the Holocene and the Arctic/North Atlantic
641 Oscillation. *Paleoceanography* 21, PA1008

642 Leng MJ, Marshall JD (2004) Palaeoclimate interpretation of stable isotope data from lake sediment
643 archives. *Quaternary Science Reviews* 23 (7-8):811-831

644 Leng MJ, Wagner B, Boehm A, Panagiotopoulos K, Vane CH, Snelling A, Haidon C, Woodley E,
645 Vogel H, Zanchetta G, Banerjee I (2013) Understanding past climatic and hydrological
646 variability in the Mediterranean from Lake Prespa sediment isotope and geochemical record
647 over the Last Glacial cycle. *Quaternary Science Reviews* 66:123-136

648 Leng MJ, Baneschi I, Zanchetta G, Jex CN, Wagner B, Vogel H (2010) Late Quaternary
649 palaeoenvironmental reconstruction from Lakes Ohrid and Prespa (Macedonia/Albania
650 border) using stable isotopes. *Biogeosciences* 7 (10):3109-3122

651 Leng MJ, Lamb AL, Heaton THE, Marshall JD, Wolfe BB, Jones MD, Holmes JA, Arrowsmith, C
652 (2005) Isotopes in lake sediments. In: Leng, MJ (ed.) *Isotopes in Palaeoenvironmental
653 Research*, Dordrecht, The Netherlands, Springer:148–176

654 Lézine AM, von Grafenstein U, Andersen N, Belmecheri S, Bordon A, Caron B, Cazet JP, Erlenkeuser
655 H, Fouache E, Grenier C, Huntsman-Mapila P, Hureau-Mazaudier D, Manelli D, Mazaud A,
656 Robert C, Sulpizio R, Tiercelin JJ, Zanchetta G, Zeqollari Z (2010) Lake Ohrid, Albania,
657 provides an exceptional multi-proxy record of environmental changes during the last glacial–
658 interglacial cycle. *Palaeogeography, Palaeoclimatology, Palaeoecology* 287 (1-4):116-127

659 Lindhorst K, Krastel S, Reicherter K, Stipp M, Wagner B, Schwenk T (2014) Sedimentary and tectonic
660 evolution of Lake Ohrid (Macedonia/Albania). *Basin Research* doi: 10.1111/bre.12063

661 Lojka R, Drábková J, Zajíc J, Sýkorová I, Franců J, Bláhová A, Grygar T (2009) Climate variability in
662 the Stephanian B based on environmental record of the Mšec Lake deposits (Kladno–
663 Rakovník Basin, Czech Republic). *Palaeogeography, Palaeoclimatology, Palaeoecology* 280
664 (1-2):78-93

665 Magny M, Vannièrè B, Zanchetta G, Fouache E, Touchais G, Petrika L, Coussot C, Walter-Simonnet
666 AV, Arnaud F (2009) Possible complexity of the climatic event around 4300-3800 cal. BP in
667 the central and western Mediterranean. *Holocene* 19 (6):823-833

668 Magny M, Bégeot C, Guiot J, Peyron O (2003) Contrasting patterns of hydrological changes in Europe
669 in response to Holocene climate cooling phases. *Quaternary Science Reviews* 22 (15-
670 17):1589-1596

671 Matter M, Anselmetti FS, Jordanoska B, Wagner B, Wessels M, Wüest A (2010) Carbonate
672 sedimentation and effects of eutrophication observed at the Kališta subaquatic springs in Lake
673 Ohrid (Macedonia). *Biogeosciences* 7 (11):3755-3767

674 Matzinger A, Schmid M, Veljanoska-Sarafiloska E, Patceva S, Guseska D, Wagner B, Müller B, Sturm
675 M, Wüest A (2007) Eutrophication of ancient Lake Ohrid: Global warming amplifies
676 detrimental effects of increased nutrient inputs. *Limnology and Oceanography* 52 (1):338-353

677 Matzinger A, Jordanoski M, Veljanoska-Sarafiloska E, Sturm M, Müller B, Wüest A (2006a) Is Lake
678 Prespa Jeopardizing the Ecosystem of Ancient Lake Ohrid? *Hydrobiologia* 553 (1):89-109

679 Matzinger A, Spirkovski Z, Patceva S, Wüest A (2006b) Sensitivity of Ancient Lake Ohrid to Local
680 Anthropogenic Impacts and Global Warming. *Journal of Great Lakes Research* 32 (1):158-
681 179

682 Meyers PA (2003) Applications of organic geochemistry to paleolimnological reconstructions: a
683 summary of examples from the Laurentian Great Lakes. *Organic Geochemistry* 34 (2):261-
684 289

685 Meyers PA, Eadie BJ (1993) Sources, degradation and recycling of organic matter associated with
686 sinking particles in Lake Michigan. *Organic Geochemistry* 20 (1):47-56

687 Meyers PA, Ishiwatari R (1995) Organic Matter Accumulation Records in Lake Sediments. In: Lerman
688 A, Imboden D, Gat J (eds) *Physics and Chemistry of Lakes*. Springer Berlin Heidelberg, pp
689 279-328

690 Meyers PA, Lallier-Verges E (1999) Lacustrine sedimentary organic matter records of Late Quaternary
691 paleoclimates. *Journal of Paleolimnology* 21 (3):345-372

692 Meyers PA, Teranes J (2001) Sediment Organic Matter. In: Last W, Smol J (eds) *Tracking
693 Environmental Change Using Lake Sediments* (2). *Developments in Paleoenvironmental
694 Research*. Springer Netherlands:239-269

695 Meyers PA, Leenheer MJ, Bourbonniere RA (1995) Diagenesis of Vascular Plant Organic Matter
696 Components during Burial in Lake Sediments. *Aquatic Geochemistry* 1:35-52

697 Panagiotopoulos K, Aufgebauer A, Schäbitz F, Wagner B (2013) Vegetation and climate history of the
698 Lake Prespa region since the Lateglacial. *Quaternary International* 293:157-169

699 Popovska C, Bonacci O (2007) Basic data on the hydrology of Lakes Ohrid and Prespa. *Hydrological
700 Processes* 21 (5):658-664

701 Pross J, Kotthoff U, Muller UC, Peyron O, Dormoy I, Schmiedl G, Kalaitzidis S, Smith AM, (2009)
702 Massive perturbation in terrestrial ecosystems of the Eastern Mediterranean region associated
703 with the 8.2 kyr B.P. climatic event. *Geology* 37 (10):887-890

704 Rasmussen SO, Vinther BM, Clausen HB, Andersen KK (2007) Early Holocene climate oscillations
705 recorded in three Greenland ice cores. *Quaternary Science Reviews* 26 (15-16):1907-1914

706 Reicherter K, Hoffmann N, Lindhorst K, Krastel S, Fernández-Steeger T, Grützner C, Wiatr T (2011)
707 Active basins and neotectonics: morphotectonics of the Lake Ohrid Basin (FYROM and
708 Albania). *Zeitschrift der Deutschen Gesellschaft für Geowissenschaften*. 162 (2):217-234

709 Reimer PJ, Bard E, Bayliss A, Beck JW, Blackwell PG, Bronk Ramsey C, Buck CE, Cheng H,
710 Edwards RL, Friedrich M, Grootes PM, Guilderson T, Hafliðason H, Hajdas I, Hatté C,
711 Heaton TJ, Hoffmann DL, Hogg AG, Hughen KA, Kaiser KF, Kromer B, Manning SW, Niu
712 M, Reimer RW, Richards DA, Scott EM, Southon JR, Staff RA, Turney CSM, van der Plicht
713 J (2013) IntCal13 and Marine13 radiocarbon age calibration curves 0–50,000 years cal BP.
714 *Radiocarbon* 55 (4):1869-1887

715 Reimer PJ, Baillie MGL, Bard E, Bayliss A, Beck JW, Blackwell PG, Ramsey CB, Buck CE, Burr GS,
716 Edwards RL, Friedrich M, Grootes PM, Guilderson TP, Hajdas I, Heaton T J, Hogg AG,
717 Hughen KA, Kaiser KF, Kromer B, McCormac FG, Manning SW, Reimer RW, Richards DA,
718 Southon JR, Talamo S, Turney CSM, van der Plicht J, Weyhenmeyer CE (2009) IntCal09 and
719 Marine09 radiocarbon age calibration curves, 0-50,000 years CAL BP. *Radiocarbon* 51
720 (4):1111-1150

721 Roberts N, Jones MD, Benkaddour A, Eastwood WJ, Filippi ML, Frogley MR, Lamb HF, Leng MJ,
722 Reed JM, Stein M, Stevens L, Valero-Garcés B, Zanchetta G (2008) Stable isotope records of
723 Late Quaternary climate and hydrology from Mediterranean lakes: the ISOMED synthesis.
724 *Quaternary Science Reviews* 27 (25-26):2426-2441

725 Roberts N, Reed JM, Leng MJ, Kuzucuoğlu C, Fontugne M, Bertaux J, Woldring H, Bottema S, Black
726 S, Hunt E, Karabiyikoğlu M (2001) The tempo of Holocene climatic change in the eastern
727 Mediterranean region: New high-resolution crater-lake sediment data from central Turkey.
728 *Holocene* 11 (6):721-736

729 Roelofs A, Kilham P (1983) The diatom stratigraphy and palaeoecology of lake Ohrid, Yugoslavia.
730 *Palaeogeography, Palaeoclimatology, Palaeoecology* 42 (3–4):225-245

731 Rohling E, Mayewski P, Abu-Zied R, Casford J, Hayes A (2002) Holocene atmosphere-ocean
732 interactions: records from Greenland and the Aegean Sea. *Climate Dynamics* 18 (7):587-593

733 Rohling EJ (1994) Review and new aspects concerning the formation of eastern Mediterranean
734 sapropels. *Marine Geology* 122 (1-2):1-28

735 Rohling EJ, Palike H (2005) Centennial-scale climate cooling with a sudden cold event around 8,200
736 years ago. *Nature* 434 (7036):975-979

737 Romanek CS, Grossman EL, Morse JW (1992) Carbon isotopic fractionation in synthetic aragonite and
738 calcite: Effects of temperature and precipitation rate. *Geochimica et Cosmochimica Acta* 56
739 (1):419-430

740 Rosenbaum J, Sheppard SMF (1986) An isotopic study of siderites, dolomites and ankerites at high
741 temperatures. *Geochimica et Cosmochimica Acta* 50 (6):1147-1150

742 Sangiorgi F, Capotondi L, Combourieu Nebout N, Vigliotti L, Brinkhuis H, Giunta S, Lotter AF,
743 Morigi C, Negri A, Reichert G-J (2003) Holocene seasonal sea-surface temperature variations
744 in the southern Adriatic Sea inferred from a multiproxy approach. *Journal of Quaternary*
745 *Science* 18 (8):723-732

746 Stankovic S (1960) *The Balkan Lake Ohrid and Its Living World* (9). *Monographiae Biologicae*.
747 Uitgeverij Dr. W. Junk, Den Haag

748 Stevens LR, Wright H.E Jr., Ito E (2001) Proposed changes in seasonality of climate during the
749 Lateglacial and Holocene at Lake Zeribar, Iran. *Holocene* 11 (6):747-755

750 Stuiver M, Reimer PJ (1993) Extended 14C data base and revised CALIB 3.0 14C age calibration
751 program. *Radiocarbon* 35 (1):215-230

752 Sulpizio R, Zanchetta G, D'Orazio M, Vogel H, Wagner B (2010) Tephrostratigraphy and
753 tephrochronology of lakes Ohrid and Prespa, Balkans. *Biogeosciences Discussions* 7
754 (3):3931-3967

755 Talbot MR (1990) A review of the palaeohydrological interpretation of carbon and oxygen isotopic
756 ratios in primary lacustrine carbonates. *Chemical Geology: Isotope Geoscience section* 80
757 (4):261-279

758 Talbot MR, Johannessen T (1992) A high resolution palaeoclimatic record for the last 27,500 years in
759 tropical West Africa from the carbon and nitrogen isotopic composition of lacustrine organic
760 matter. *Earth and Planetary Science Letters* 110 (1-4):23-37

761 Talbot MR, Kelts K (1990) Paleolimnological signatures from carbon and oxygen isotopic ratios in
762 carbonates from organic carbon-rich lacustrine sediments. In: Katz, BJ (ed.) *Lacustrine basin*
763 *exploration*:99-112

764 Talbot MR, Livingstone DA (1989) Hydrogen Index and Carbon Isotopes of Lacustrine Organic-
765 Matter as Lake Level Indicators. *Palaeogeography Palaeoclimatology Palaeoecology* 70 (1-
766 3):121-137

767 Törnqvist TE, Hijma MP (2012) Links between early Holocene ice-sheet decay, sea-level rise and
768 abrupt climate change. *Nature Geoscience* 5 (9):601-606

769 Usdowski E, Hoefs J (1990) Kinetic $^{13}\text{C}/^{12}\text{C}$ and $^{18}\text{O}/^{16}\text{O}$ effects upon dissolution and outgassing of
770 CO_2 in the system $\text{CO}_2/\text{H}_2\text{O}$. *Chemical Geology: Isotope Geoscience Section* 80 (2):109-118

771 Van Geel B, Heusser CJ, Renssen H, Schuurmans CJE (2000) Climatic change in Chile at around 2700
772 BP and global evidence for solar forcing: A hypothesis. *Holocene* 10 (5):659-664

773 Vogel H, Wagner B, Zanchetta G, Sulpizio R, Rosén P (2010a) A paleoclimate record with
774 tephrochronological age control for the last glacial-interglacial cycle from Lake Ohrid,
775 Albania and Macedonia. *Journal of Paleolimnology* 44 (1):295-310

776 Vogel H, Zanchetta G, Sulpizio R, Wagner B, Nowaczyk N (2010b) A tephrostratigraphic record for
777 the last glacial-interglacial cycle from Lake Ohrid, Albania and Macedonia. *Journal of*
778 *Quaternary Science* 25 (3):320-338

779 Wagner B, Wilke T, Krastel S, Zanchetta G, Sulpizio R, Reicherter K, Leng M, Grazhdani A,
780 Trajanovski S, Levkov Z, Reed J, Wonik T (2014) More Than One Million Years of History
781 in Lake Ohrid Cores. *EOS* 95 (3):25-26

782 Wagner B, Francke A, Sulpizio R, Zanchetta G, Lindhorst K, Krastel S, Vogel H, Rethemeyer J, Daut
783 G, Grazhdani A, Lushaj B, Trajanovski S (2012) Possible earthquake trigger for 6th century
784 mass wasting deposit at Lake Ohrid (Macedonia/Albania). *Climate of the Past* 8 (6):2069-
785 2078

786 Wagner B, Vogel H, Zanchetta G, Sulpizio R (2010) Environmental change within the Balkan region
787 during the past ca. 50 ka recorded in the sediments from lakes Prespa and Ohrid.
788 *Biogeosciences* 7 (10):3187-3198

789 Wagner B, Lotter AF, Nowaczyk N, Reed JM, Schwalb A, Sulpizio R, Valsecchi V, Wessels M,
790 Zanchetta G (2009) A 40,000-year record of environmental change from ancient Lake Ohrid
791 (Albania and Macedonia). *Journal of Paleolimnology* 41 (3):407-430

792 Wagner B, Reicherter K, Daut G, Wessels M, Matzinger A, Schwalb A, Spirkovski Z, Sanxhaku M
793 (2008a) The potential of Lake Ohrid for long-term palaeoenvironmental reconstructions.
794 *Palaeogeography, Palaeoclimatology, Palaeoecology* 259 (2-3):341-356

795 Wagner B, Sulpizio R, Zanchetta G, Wulf S, Wessels M, Daut G, Nowaczyk N (2008b) The last 40 ka
796 tephrostratigraphic record of Lake Ohrid, Albania and Macedonia: a very distal archive for
797 ash dispersal from Italian volcanoes. *Journal of Volcanology and Geothermal Research* 177
798 (1):71-80

799 Wanner H, Beer J, Bütikofer J, Crowley TJ, Cubasch U, Flückiger J, Goosse H, Grosjean M, Joos F,
800 Kaplan JO, Küttel M, Müller SA, Prentice IC, Solomina O, Stocker TF, Tarasov P, Wagner
801 M, Widmann M (2008) Mid- to Late Holocene climate change: an overview. *Quaternary
802 Science Reviews* 27 (19-20):1791-1828

803 Wick L, Lemcke G, Sturm M (2003) Evidence of Lateglacial and Holocene climatic change and human
804 impact in eastern Anatolia: High-resolution pollen, charcoal, isotopic and geochemical records
805 from the laminated sediments of Lake Van, Turkey. *Holocene* 13 (5):665-675

806 Zanchetta G, Van Welden A, Baneschi I, Drysdale R, Sadori L, Roberts N, Giardini M, Beck C,
807 Pascucci V, Sulpizio R (2012) Multiproxy record for the last 4500 years from Lake Shkodra
808 (Albania/Montenegro). *Journal of Quaternary Science* 27 (8):780-789

809 Zanchetta G, Borghini A, Fallick AE, Bonadonna FP, Leone G (2007a) Late Quaternary
810 palaeohydrology of Lake Pergusa (Sicily, southern Italy) as inferred by stable isotopes of
811 lacustrine carbonates. *Journal of Paleolimnology* 38 (2):227-239

812 Zanchetta G, Drysdale RN, Hellstrom JC, Fallick AE, Isola I, Gagan MK, Pareschi MT (2007b)
813 Enhanced rainfall in the Western Mediterranean during deposition of sapropel S1: stalagmite
814 evidence from Corchia cave (Central Italy). *Quaternary Science Reviews* 26 (3-4):279-286

Figure 1

[Click here to download Figure: Figure 1.pdf](#)

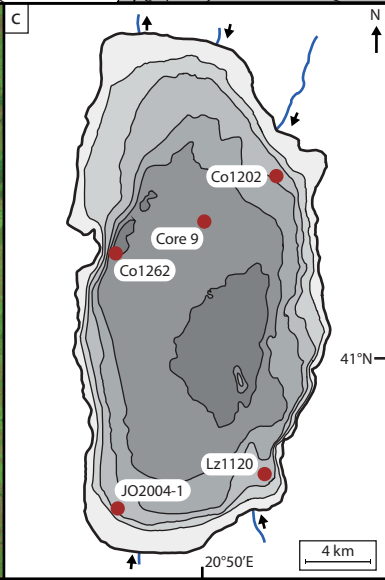
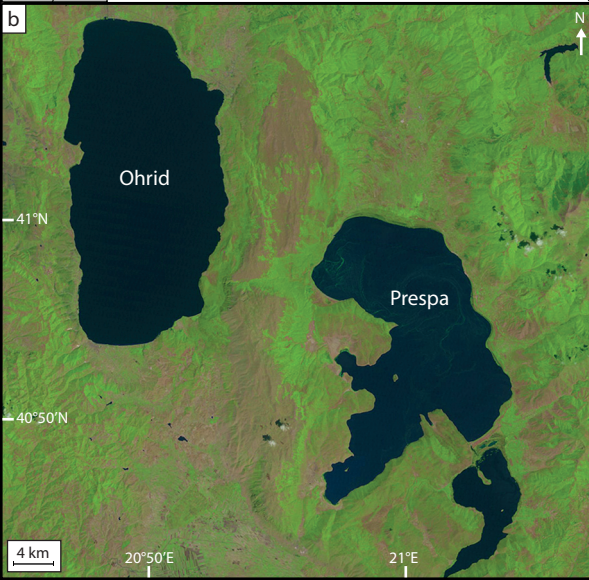
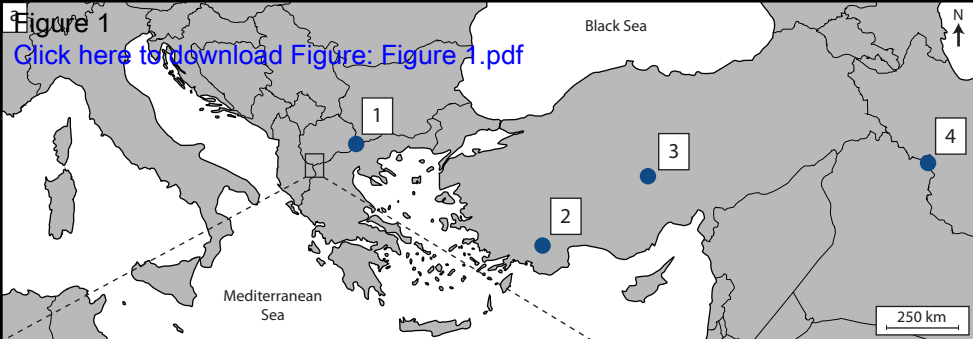


Figure 2

[Click here to download Figure: Figure 2.pdf](#)

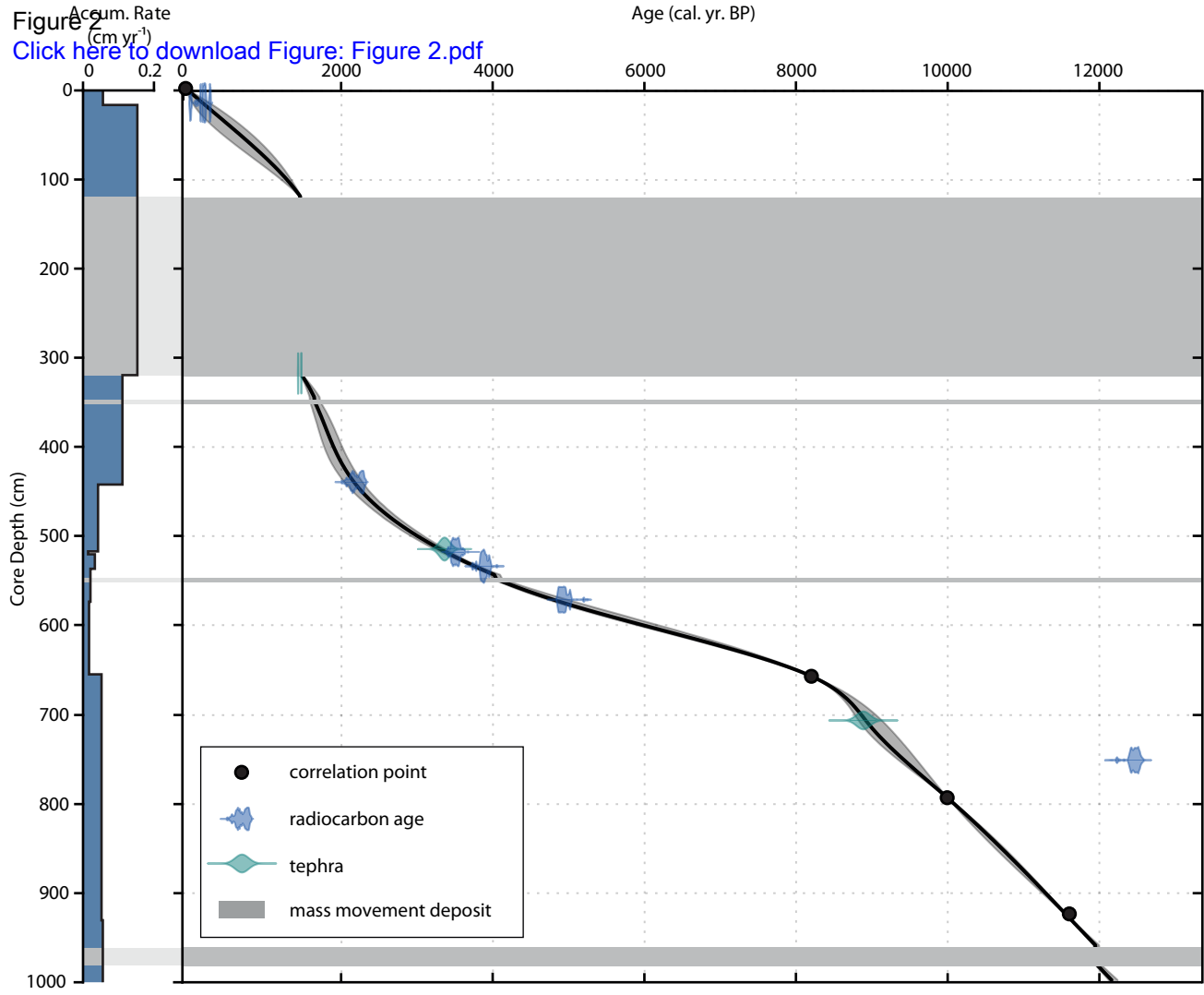


Figure 4

[Click here to download Figure: Figure 4.pdf](#)

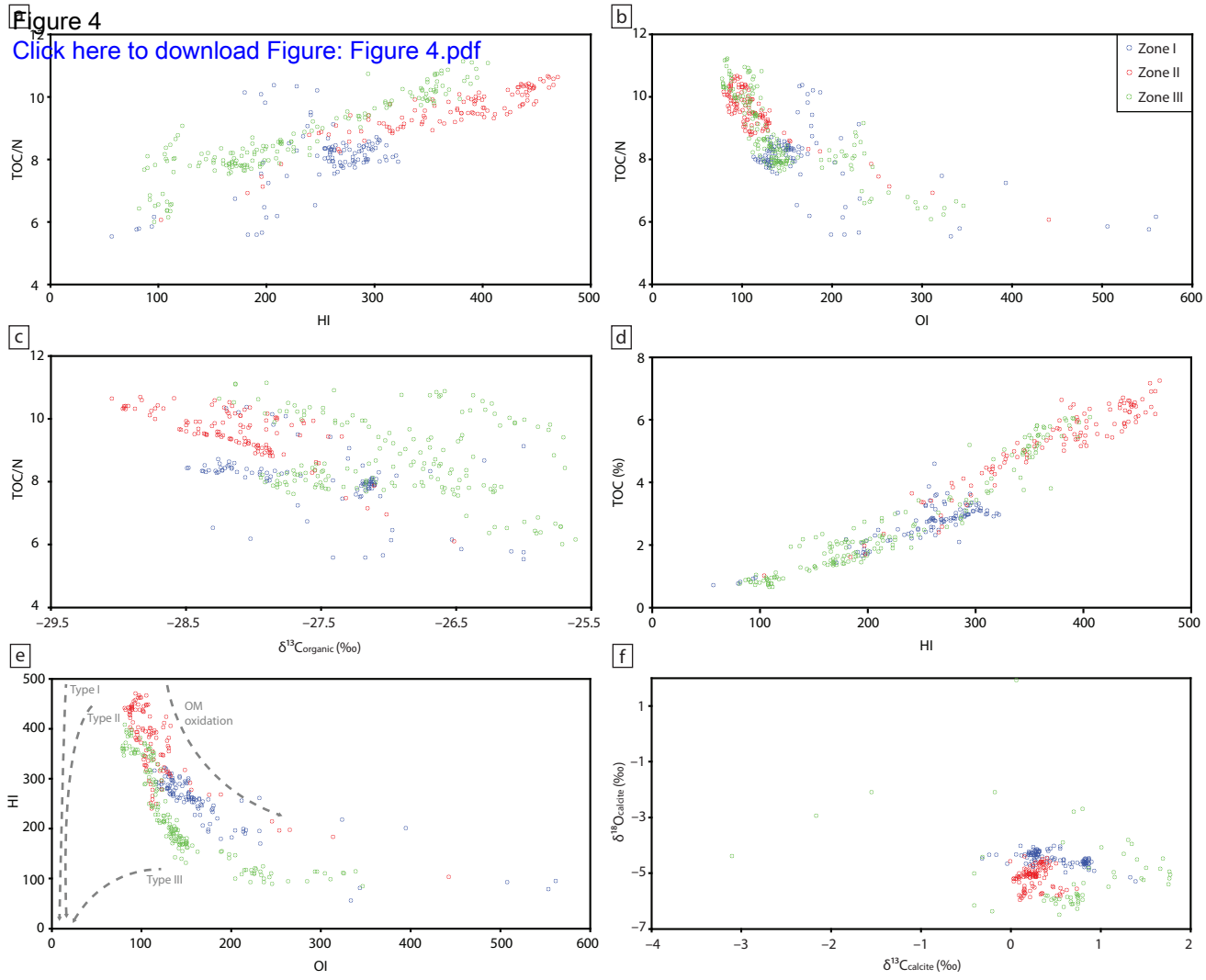


Figure 5

[Click here to download Figure: Figure 5.pdf](#)

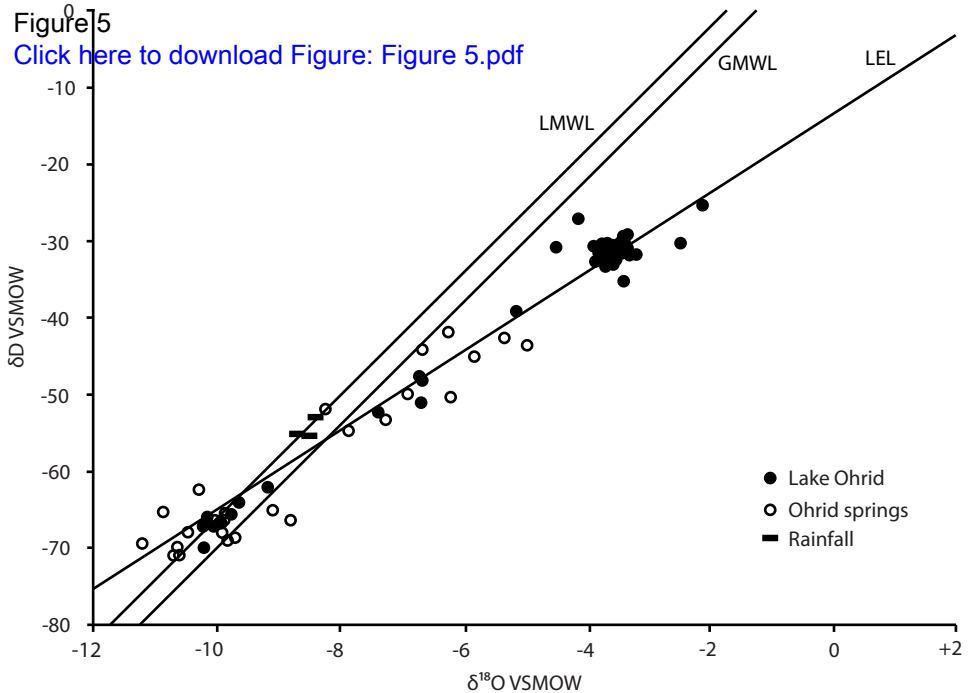


Figure 6

[Click here to download Figure: Figure 6.pdf](#)

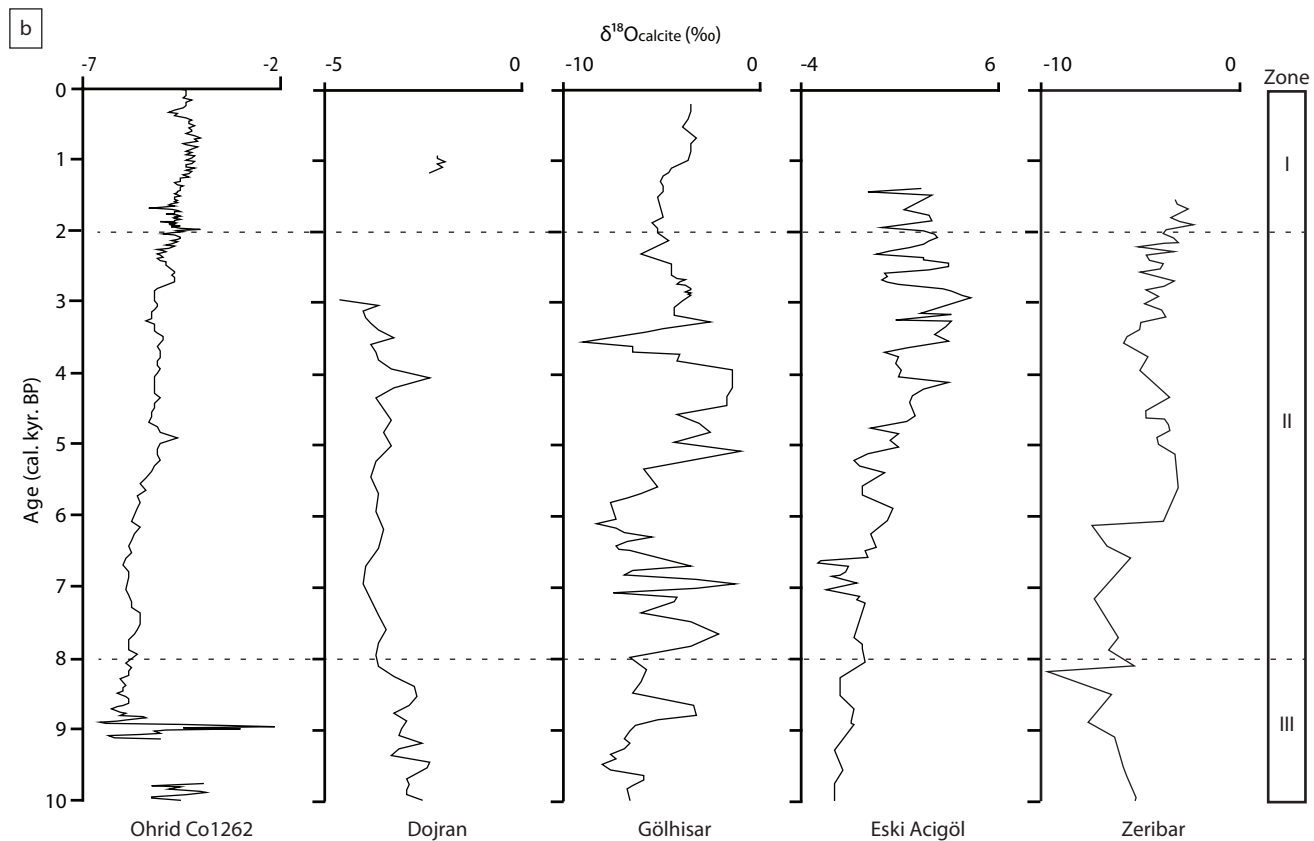
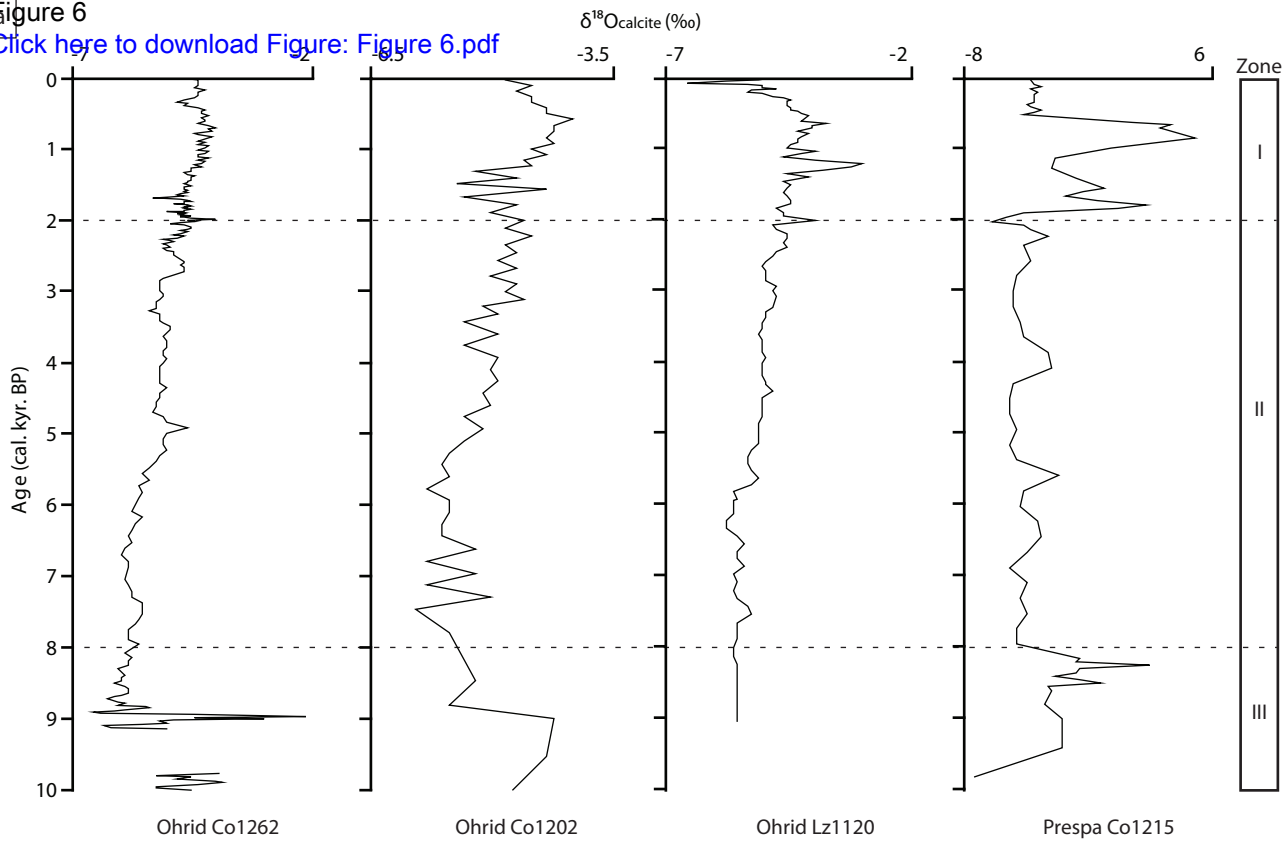


Table 1

| Core depth (cm) | Material | Age (cal. yr. BP) |
|------------------------|----------------------------------|--------------------------|
| 17 | terrestrial plant | 140 ±145 |
| 320 | Somma-Vesuvius AD 472/512 tephra | 1478/1438 ¹ |
| 442 | terrestrial plant | 2190 ±140 |
| 517 | Etna FL tephra | 3370 ±70 ² |
| 520 | terrestrial plant | 3510 ±110 |
| 537 | terrestrial plant | 3850 ±130 |
| 574 | terrestrial plant | 5030 ±190 |
| 709 | Mercato tephra (glass shards) | 8530 ±100 ³ |
| 754 | fish bone | 12400 ±190 |

¹Vogel et al. (2010b), ²Coltelli et al. (2000), ³Zanchetta et al. (2011)

Table 2

| Fig.4 | Proxy | Zone I | Zone II | Zone III | Whole Core |
|--------------|---|---------------|----------------|-----------------|-------------------|
| a | TOC/N - HI | 0.23 | 0.84 | 0.86 | 0.64 |
| b | TOC/N - OI | 0.25 | 0.72 | 0.59 | 0.51 |
| c | TOC/N - $\delta^{13}\text{C}_{\text{organic}}$ | 0.20 | 0.63 | 0.06 | 0.17 |
| d | TOC - HI | 0.70 | 0.91 | 0.92 | 0.92 |
| e | HI - OI | 0.69 | 0.55 | 0.65 | 0.48 |
| f | $\delta^{18}\text{O}_{\text{calcite}} - \delta^{13}\text{C}_{\text{calcite}}$ | 0.35 | 0.00 | 0.05 | 0.02 |